DoppleSleep: A Contactless Unobtrusive Sleep Sensing System Using Short-Range Doppler Radar

Tauhidur Rahman[1], **Alexander T. Adams**[1], **Ruth Vinisha Ravichandran**[2], **Mi Zhang**[3], **Shwetak N. Patel**[2], **Julie A. Kientz**[2], **Tanzeem Choudhury**[1]
[1]Cornell University, [2]University of Washington, [3]Michigan State University
tr266@cornell.edu, ata56@cornell.edu, vinisha@uw.edu, mizhang@msu.edu, shwetak@uw.edu, jkientz@uw.edu, tkc28@cornell.edu

ABSTRACT
In this paper, we present DoppleSleep – a contactless sleep sensing system that continuously and unobtrusively tracks sleep quality using commercial off-the-shelf radar modules. DoppleSleep provides a single sensor solution to track sleep-related physical and physiological variables including coarse body movements and subtle and fine-grained chest, heart movements due to breathing and heartbeat. By integrating vital signals and body movement sensing, DoppleSleep achieves 89.6% recall with Sleep vs. Wake classification and 80.2% recall with REM vs. Non-REM classification compared to EEG-based sleep sensing. Lastly, it provides several objective sleep quality measurements including sleep onset latency, number of awakenings, and sleep efficiency. The contactless nature of DoppleSleep obviates the need to instrument the user's body with sensors. Lastly, DoppleSleep is implemented on an ARM microcontroller and a smartphone application that are benchmarked in terms of power and resource usage.

Author Keywords
Sleep Sensing; Doppler radar; Vital Sign Monitoring

ACM Classification Keywords
C.3 Special-Purpose and Application-Based Systems: Signal Processing Systems

General Terms
Algorithm, Design, Experimentation, Measurement

INTRODUCTION
Consuming almost a third of our daily lives, sleep is a significant marker of an individual's health and well-being. Getting ample, good-quality sleep facilitates higher levels of productivity, mental performance, and physical growth [11]. However, a majority of the general population remains unaware of their overall sleep quality or longer-term patterns in their sleep duration and consistency [37]. Some people suspected of having sleep disorders such as sleep apnea or narcolepsy may be advised by physicians to undergo sleep studies in a laboratory, which consists of a single, highly studied night. However, many people with poor sleep quality have more long-term sleep issues such as insomnia or delayed sleep phase syndrome that require longer term monitoring to diagnose, monitor, and treat. A sleep monitoring system that can unobtrusively and objectively measure sleep quality over the long term could provide users with valuable insights into their sleep habits, help them take corrective measures such as improving their sleep hygiene, and ultimately help with identifying more sleep disorders, which often go undiagnosed.

Apart from short-term diagnostic systems like polysomnography, there is a wide variety of commercial long-term sleep monitoring devices. An overview of the state of art in sleep sensing can inform us of the existing gaps in the practical usage of sleep sensing systems. At one end of the spectrum is polysomnography (PSG), which is regarded as the medical gold standard for assessing sleep quality and for diagnosing sleep-related disorders such as sleep apnea [15]. By instrumenting patients with at least 7 different sensors and electrodes that track various sleep-related physiological parameters throughout the night, PSG provides fine-grained sleep quality assessment. PSG is considered a highly obtrusive sleep sensing system due to its expense, impracticality for home-based use, and comfort-level for the patient, and thus its application is limited to diagnosing sleep-related disorders in clinical settings for short durations. At the other end of the spectrum are commercial devices that enable long-term sleep monitoring. These primarily use Actigraphy, a widely adopted method that infers sleep duration and quality by measuring body motion during sleep [18]. Numerous consumer electronic fitness trackers [8, 3] leverage inbuilt accelerometers to provide actigraphy based sleep monitoring. However, many users are resistant to the idea of having to wear or place sensors close to the body during sleep [17]. To facilitate non-contact sensing, smartphone apps have been developed that sense sleep-related environmental factors in addition to body movement to infer sleep quality. A low-cost, long-term, contactless sleep sensing system that monitors sleep related physiological variables similar to PSG but with the unobtrusiveness and potential for long-term monitoring of actigraphy could bridge the gap between effectiveness and daily usage of sleep sensing.

UbiComp '15, September 7–11, 2015, Osaka, Japan.

http://dx.doi.org/10.1145/2750858.2804280

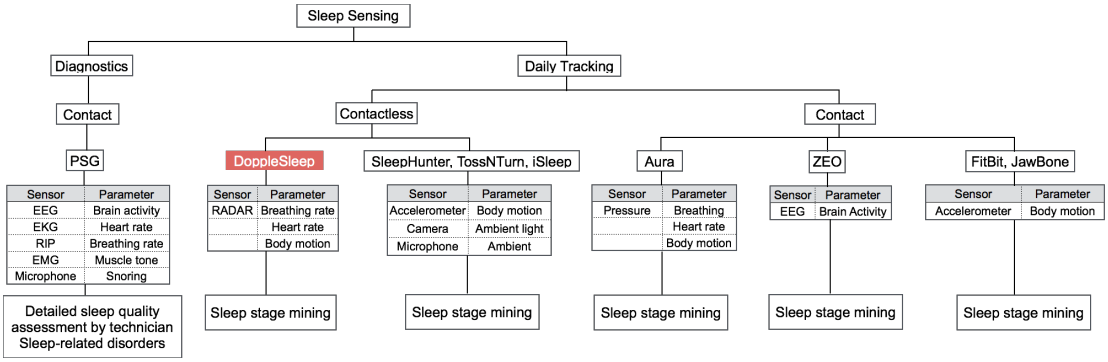

Figure 1: Comparison of DoppleSleep with a few state of the art sleep sensing technologies in terms of their typical usage, intrusiveness, affordances, sensing modalities, captured sleep biomarkers and predicted sleep variables.

In this paper, we present DoppleSleep, a contactless sleep sensing technology that monitors three significant sleep-related biomarkers: breathing rate, heart rate, and body motion using a single, low-cost, off-the-shelf, K-band 24GHz radar module. Using a radar transceiver, the system tracks phase changes in the reflected electromagnetic waves and tracks the sleeper's body and limb movements. In the absence of large body movements, it also estimates the sleeper's breathing and heart rate using the periodic phase changes of the reflected wave from the expansion and contraction of heart and chest wall. DoppleSleep's breathing and heart rate estimation algorithm is relatively robust at various orientations and distances up to 2m between the user's body and sensor. It can estimate heart and breathing rate with an overall mean absolute error of 1.98 and 3.29 cycles per minute respectively. DoppleSleep uses these three sleep biomarkers to classify an epoch (the time unit for sleep classification) as a sleep or wake event with a recall of 89.6%. The sleep events are further classified as REM or NREM sleep stages with a recall of 80.2%. Lastly DoppleSleep objectively quantifies sleep quality using validated measures like sleep onset latency, number of awakenings, total sleep time, and sleep efficiency, similar to those produced in a PSG report [6]. DoppleSleep is comprised of an embedded system unit and a smartphone application unit. The embedded system unit locally samples and amplifies the raw radar baseband signal and transmits the signal to the smartphone via Bluetooth for further processing. The smartphone application unit is then used for heart rate, breathing rate, movement estimation, and sleep modeling. Although contactless detection of vital signals has been explored and refined over the last several decades, this is the first attempt that uses vital signals for sleep stage mining. The specific contributions of this paper are as follows:

1. A novel and complementary approach to sleep measurement that does not require contact with the user or the user's bed.
2. Evaluation of the contactless sensing of physical movements, heart rate, and breathing rate using short-range Doppler radar in both laboratory and real world settings.
3. Development and preliminary validation of Sleep vs. Wake and REM vs. Non-REM classification and objective sleep quality measurements on about 110 hours of sleep data collected from 16 sleep sessions with 8 participants.
4. Implementation and benchmarking of the signal processing and machine learning algorithm on an ARM microcontroller and an Android smartphone.

RELATED WORK

Polysomnography (PSG), which is considered as the "medical gold standard" of sleep sensing [15], is performed in a controlled environment such as a sleep lab and is used to diagnose sleep-related breathing disorders like sleep apnea as well as other disorders such as narcolepsy, idiopathic hypersomnia, periodic limb movement, or parasomnias. In PSG, patients have electrodes and sensors attached to them that monitor physiological functions such as electrical activity of the brain, heart rate, respiration rate, oxygen saturation, limb movements, and eye movements during sleep. A sleep technician then scores the data, typically collected over a single night, using various criteria to assess sleep quality. PSG is limited to short-term sleep sensing since it is performed in a lab and thus may not be an accurate representation of a patient's typical sleep habits. The WatchPAT [10] is one of the few portable wearable sleep apnea diagnostic tools that continuously monitors peripheral arterial tone (PAT) and changes in the autonomic nervous system during sleep outside of a lab setting. Although WatchPAT allows users to diagnose sleep apnea from the comfort of their homes, it is still considered obtrusive due to its comparatively large form factor combined with the fact that the users will have to wear the device for an average of 8 hours each night.

Since EEG has been established as an accurate method to monitor sleep stages [21, 25], commercial sleep sensors like the Zeo [7] assess sleep quality by measuring electrical activity in the brain. Users are required to wear a band embedded with three EEG sensors around the forehead while sleeping. Although less obtrusive than PSG, this is may still be considered cumbersome and may interfere with the natural sleeping habits of the user, as many are reluctant to wear sensors to bed on a regular basis [17]. For this reason, other less-invasive commercial alternatives have been developed.

Actigraphy infers sleep quality by measuring human motor movements [36]. Because body movement can be easily

measured from an accelerometer placed in a user's vicinity, actigraphy based sleep sensing can be done non-intrusively either using commercial fitness bands like the fitbit [8], jawbone up [3], or using a smart phone: all devices that have built-in accelerometers. The raw accelerometer data is continuously sampled to detect coarse body movements such as tossing and turning during sleep and marks these as arousal events. However, it still requires the user to either place a smartphone in their vicinity or wear a wristband while sleeping. Another drawback is that by inferring sleep quality by tracking only a single physiological factor, actigraphy tends to overestimate or underestimate certain sleep parameters like sleep onset latency, total sleep time and sleep efficiency [18]. In addition, clinicians believe actigraphy is only accurate for normal adults with relatively good sleep patterns [35], which limits its use in children, older adults, or people suspected of sleep disorders, which is a large percentage of the target population for sleep sensing.

To facilitate non-contact sleep sensing, several groups in the research community have proposed systems that indirectly assess sleep quality by measuring factors related to the sleep environment, Kay et al. [26] proposed Lullaby, a capture and access system that tracks various factors in the environment that affects sleep quality using a suite of temperature, light, sound, motion and an off-the shelf sleep sensor to help identify potential sleep disruptors. More recently, researchers have leveraged existing sensors in a smartphone to do the same. Hao et al. proposed iSleep [24], which leverages a smartphone's built-in microphone to unobtrusively measure sound caused by body movement, cough, and snoring. Gu et al. [22] proposed Sleep Hunter, a system that uses the smartphone's microphone, accelerometer, light sensor, etc. to capture both environmental disturbances (light, noise etc.) and human physiological reactions (like movements, cough, snore etc.) to model different stages of sleep (e.g., REM, deep, and light sleep). Sleep is considered as a private activity in our everyday life [26], and thus recording audio and video information throughout the night, although contactless and online, might still be considered obtrusive in terms of privacy and comfort.

Research from the medical community has shown that vital signals vary depending on sleep stages, including wakefulness, REM, and Non-REM [2]. Therefore, variability in vital signals such as breathing and heart rate can be used as indicators of transition into different sleep stages. A recent commercially available sensor, Aura[13], tracks both movements and vital signals using pressure pad on the users's bed. In this paper, our proposed sleep sensing system uses a short-range doppler radar module to track the user's vital signals such as heart beat and breathing along with coarse body movements unobtrusively while sleeping. By detecting variations in vital signals and body movement, our mobile system then classifies different stages of sleep and assesses sleep quality. Due to the contact-free nature of the radar module, our mobile system alleviates users from the physical burden of wearing a sensor. The absence of any audio-visual recording mitigates privacy concerns. Figure 1 outlines the contribution of DoppleSleep and compares with other sleep sensing technologies.

TRACKING SLEEP BIOMARKERS USING DOPPLESLEEP

Here we describe the techniques of tracking human physical movement, heart rate and breathing rate using a single short-range Doppler radar. We then report the feasibility of our system in a controlled study in laboratory settings.

Fundamentals of Doppler Radar

The concept of contactless vital signal monitoring using microwave signals has been explored since the 1970s [32]. Since then a lot of research has been done to improve the performance of the system both in analog circuit design of high frequency carrier signal as well as signal processing of base-banded signal. Different choices of radio frequencies have been explored starting from 1150 MHz to detect vitals through earthquake rubble and concrete [16] all the way up to Ka band [39] to improve detection sensitivity. Different receiver architectures [31] and techniques to compensate for phase noise [29] have been proposed and tested. Over the years, RADAR modules have been reduced from bulky military grade systems mounted on a tripod to a relatively small BiCMOS chips suitable for integration in portable electronic devices [20]. A comprehensive study on RADAR technology for vital signal detection can be found in [27]. Building on top of this massive prior knowledge, DoppleSleep explores the feasibility of contactless vital sensing using RADAR in the sleep-sensing domain. We selected a K band (24 GHz) direct conversion quadrature RADAR module, as it was most suitable for our application.

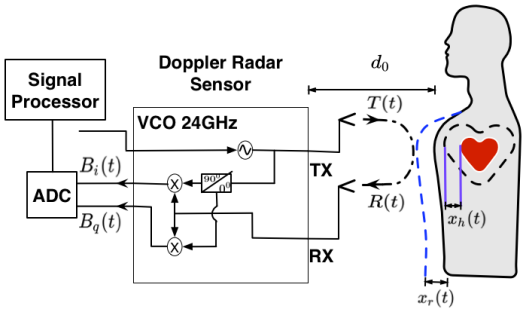

Figure 2: Detection theory of heartbeat and breathing using continuous wave (CW) Doppler radar.

The fundamental principle behind detecting vital signals using continuous wave (CW) Doppler radar is demonstrated in figure 2. The module transmits a single tone $T(t)$ on a carrier frequency of f, wavelength of $\lambda = c/f$, combined with phase noise $\phi(t)$ from the oscillator, given by the equation (1):

$$T(t) = \cos(2\pi ft + \phi(t)) \tag{1}$$

Assume that $T(t)$ traverses a distance of d_0 and hits a human's body generating periodic chest movements due to respiration and heart beating. If the displacement of chest due to respiration is $x_r(t)$ and the displacement of heart due to heart beat is $x_h(t)$, the overall movement can be expressed

as $x(t) = x_r(t) + x_h(t)$. As a result, the reflected signal $R(t)$ received by the radar is given by:

$$R(t) \approx A_r \cos(2\pi ft - \frac{4\pi d_0}{\lambda} - \frac{4\pi x(t)}{\lambda} + \phi(t - \frac{2d_0}{c})) \quad (2)$$

$R(t)$ is a time delayed and amplitude reduced version (reduced to A_r) of the transmitted signal $T(t)$. Most importantly, the information of $x(t)$ is phase modulated in $R(t)$ in addition to the distance between the human body and the radar, d_0 and a time delayed version of the phase noise $\phi(t - \frac{2d_0}{c})$. After $R(t)$ goes through a Low Noise Amplifier (LNA), it is converted to baseband by a mixer that multiplies the received signal with a copy of the transmitted signal. The output of the mixer gives the difference or intermediate frequencies (IF). The receiver thus gets rid off any information related to carrier frequency ($2\pi ft$) and preserves the change in phase of the signal corresponding to $x(t)$ which we want to capture. In this study we use a quadrature receiver, which compensates for null detection points a problem faced by single channel receivers [19]. In a quadrature receiver, $R(t)$ is split into two components and multiplied by two copies of transmitted signal that are 90^o out of phase with each other. The output is thus a pair of orthonormal baseband signals, $B_I(t)$ and $B_Q(t)$, expressed by equation 3.

$$\begin{aligned} B_i(t) &= \cos(\theta + \frac{\pi}{4} + \frac{4\pi x(t)}{\lambda} + \Delta\phi(t)) \\ B_q(t) &= \cos(\theta - \frac{\pi}{4} + \frac{4\pi x(t)}{\lambda} + \Delta\phi(t)) \end{aligned} \quad (3)$$

Here, $\theta = 4\pi d_0/\lambda + \theta_0$, contains the target distance information d_0. and $\Delta\phi(t)$ is the residual oscillator phase noise. The portion of interest is therefore the phase modulation due to physical and physiological movements $x(t)$ given by $\frac{4\pi x(t)}{\lambda}$. Since $B_I(t)$ and $B_Q(t)$ have a 90^o phase difference, the quadrature receiver ensures that atleast one of the baseband channels is not at a null detection point [19]. For example, if the distance d_0 that makes up θ is such that θ is $\pi/4$, then $B_i(t)$ and $B_q(t)$ can be approximated as

$$\begin{aligned} B_i(t) &\approx \frac{4\pi x(t)}{\lambda} + \Delta\phi(t) \\ B_q(t) &\approx 1 - [\frac{4\pi x(t)}{\lambda} + \Delta\phi(t)]^2 \end{aligned} \quad (4)$$

Here $B_i(t)$ is at an optimal point with full sensitivity, while $B_q(t)$ is at a null point with least sensitivity. Thus phase information can be recovered from one channel even if the other is at a null point. The next step is to process the two channels to get a output signal that is compensated for null-point. There are various null-point compensation techniques including frequency tuning technique [38], complex signal demodulation [28] and arctangent demodulation [34]. In this study we used a simpler technique of selecting one optimal channel that is farthest from the null point using interquartile range. Higher interquartile range of a channel will indicate that it is further away from the null-point, thus the optimal channel.

Sensing Physical Movements

During sleep, out body manifests voluntary body movements such as tossing and turning, changing posture and involuntary limb movements such as myoclonic twitches [2]. The frequency and extent of the physical movements and vital signal variations during sleep can be used as indicators of sleep quality. Now we explain the algorithm used to segment physical movements during sleep.

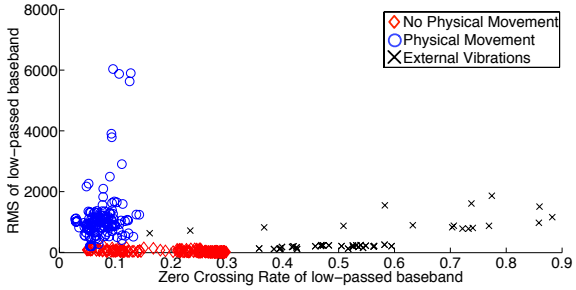

Figure 3: The scatter plot of no physical movement, physical movement and external vibrations in a two-dimensional feature space formed by frame-level RMS energy and zero crossing rate of the low passed signal (cutoff 3Hz) of the optimal channel.

The challenge of using Doppler radar to track physical movements is that we must be able to isolate noise due to vibrations from appliances such as fan, air-conditioning unit or a speaker within the radar's range from human body movements. In order to address this challenge, we recorded physical activity data using the radar module and an accelerometer in our lab with 4 subjects. We then simulated three scenarios: (a) no physical movement, (b) common sleep related body movements (e.g. leg movements, tossing and turning, sitting up, head movements) and, (c) environmental noise induced by appliances. This was used as training data for our motion classifier. We then applied a low pass filter with cut off frequency at 3Hz, on the baseband signal, to remove high frequency periodic noise caused by environmental factors. As a result the frame-level RMS energy of the filtered baseband signal mostly corresponds to the presence or absence of body movements (figure 3). However, there may be some frames where relatively high RMS energy may be caused due to aperiodic changes in the machine (e.g when the machine switches) (figure 3). In order to isolate these frames, the zero-crossing rate and the RMS energy of the filtered baseband signal are used as features for every 30 second frame. A leave-one-subject-out cross-validation experiment with a very simple threshold-based classifier indicates that these two features extracted in a frame level can easily discriminate among the three categories with an average recall of 94.5%. Using our algorithm to detect human movement, we found that the frame-level RMS energy of the filtered baseband signal is correlated (mutual information 0.86) with

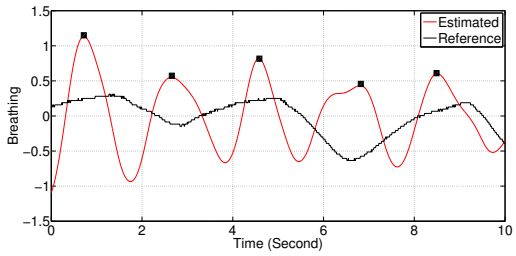

(a)

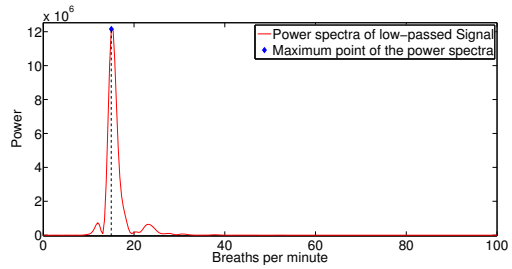

(b)

Figure 4: (a) shows the estimated and the reference breathing waveform, (b) shows the power spectral density of the estimated breathing waveform.

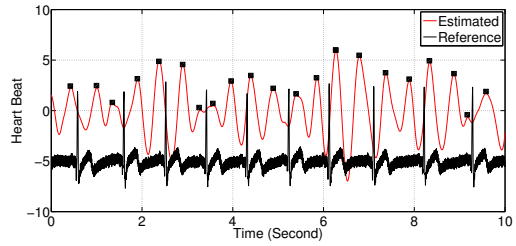

(a)

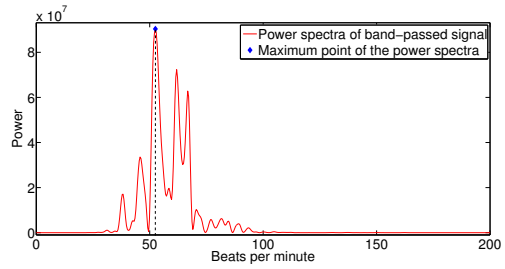

(b)

Figure 5: (a) shows the estimated and the reference heart beat waveform (b) shows the power spectral density of the estimated heart beat waveform.

the frame-level RMS energy of the norm of 3D acceleration values from the accelerometer worn by our participants.

Sensing Breathing and Heart Rate

Once the signal frames containing movement data have been classified and isolated, we then proceed to estimate breathing and heart rate on frames that contain no body movement. As explained previously, the baseband signal $B_i(t)$ is a linear combination of movement caused by breathing and heart beat signal ($x(t) = x_h(t) + x_r(t)$). As the breathing process generates relatively lower frequency signals than the heart beating process, we used two bandpass filters to isolate x_h and $x_r(t)$ from $B_i(t)$. The bandpass filter for estimating breathing rate captures the lower frequencies that gets created in the baseband signal due to chest expansion and contraction. Specifically, we used a minimum order Butterworth filter with stop-band frequencies at 0.1 Hz, 0.8 Hz and passband frequencies at 0.3 Hz, 0.7 Hz to estimate any breathing rate ranging between 9 and 20 Breath per Minute. Similarly another minimum order band-pass Butterworth filter was designed with stop-band frequencies at 1 Hz, 3 Hz and passband frequencies at 1.5 Hz, 2.5 Hz to estimate any heart rate between about 45 and 80 Beat per Minute. For both filters, passband ripple and stop-band attenuation was chosen to be 1 dB and 60 dB respectively. These Butterworth filters have proven to be useful for vital sign estimation in prior literature [33]. These two filters are applied on the baseband signal $B_i(t)$ to get the estimated breathing and heartbeat waveform. Figure 4a shows the estimated and reference (or ground truth) breathing waveform from a respiratory inductance plethysmography (RIP) band. Similarly, figure 5a shows the estimated heartbeat waveform overlaid with the reference heartbeat signal from an electrocardiogram (ECG).

In figure 4a, the peaks and troughs of the reference signal correspond to inhalation and exhalation. Notice that the estimated breathing waveform has peaks in both peaks and troughs of the reference signal. Hence, for every cycle of the reference breathing signal, we get about two cycles of our estimated breathing signal, one for inhalation and the other for exhalation. Thus the estimated breathing rate is half the frequency of the filtered signal. By applying a Fourier transform on the filtered baseband signal, we can then estimate the power spectral density of the signal as illustrated in figure 4b. The peak of the power spectral density corresponds to the dominant frequency, which is in this case the breathing rate. Similarly in figure 5a, for every cycle of the reference heart beat signal, we get two cycles of our estimated heart beat signal. Thus the estimated heart rate is half the frequency of the filtered signal. Figure 5b shows the power spectral density of the estimated heart beat, where the peak corresponds to the dominant frequency, which is the heart rate. In order to smooth our heart and breathing rate estimation, we applied a moving average filter with a length of 16. We also found that the window size of 30 seconds and shift of 5 seconds minimizes the heart rate and breathing rate estimation error.

For a sleep sensing system to work in real-world settings the vital signal tracking needs to be robust to relative orientation and distance between the radar sensor and the users' bodies during sleep. In order to evaluate the performance of DoppleSleep at various orientations and distances, we conducted two studies in a controlled environment. Four participants were recruited and their breathing and heart rate was recorded using the radar modules placed at different distances and orientation. The reference heart and breathing rates was recorded from a biometric shirt Hexoskin [9],

embedded with an electrocardiogram (ECG) to provide heart rate value and respiratory inductance plethysmography (RIP) to provide breathing rate value. Comparing the estimated heart and breathing rates to the reference values we computed the mean absolute error.

Distance Test

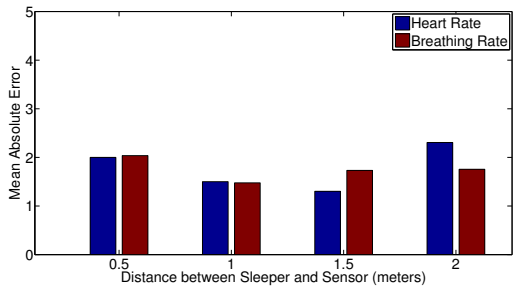

Figure 6: The performance of the heart and breathing rate estimation algorithm across different distances in terms of mean absolute error measured in cycles (beats or breaths) per minute (CPM).

The distance d_0 between the subject and the radar is directly correlated to the power of the reflected $R(t)$ and the baseband signals B_I, B_Q. Specifically, as the distance d_0 increases, the reflected signal gets weaker ($A_r \rightarrow 0$ in equation 2) due to signal loss when propagating through the longer distance. The aim of this test was to find out the effect of distance on DoppleSleep's heart and breathing rate detection algorithm. We recruited 4 subjects and asked them to lie down in a supine position in our laboratory. We then varied the distance between the Radar and the subject from 0.5m to 2m with 0.5m increments. Figure 6 illustrates the mean absolute error of heart and breathing rate estimation for different distances. We can observe that as distance increases the estimation error for both heart and breathing rate slightly increases as we expected. However the overall error rate stays within 2 CPM for distances up to 2m.

Orientation Test

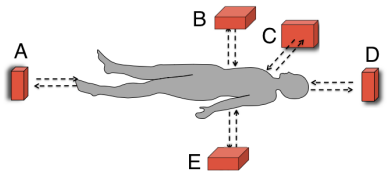

Figure 7: The setup of the orientation test where heart and breathing rates are estimated with a radar in five different orientations with respect to the body: (A) facing the bottom of the feet, (B) facing the chest, (C) facing the side of the torso, (D) facing the top of the head and (E) facing the back.

The orientation test was conducted to explore the effect of relative orientation of the radar sensor with respect to the user's body, on heart and breathing rate estimation. Different orientations allow the sensor to capture different profiles of the human body as the heart and chest wall compress and expand. Thus different orientations may result in different error rates for heart and breathing rate estimation. Figure 7 illustrates the setup of the test conducted with 4 participants in a laboratory setting. We estimated heart and breathing rates using the radar at five different orientations with respect to the subject's body: (A) facing the bottom of the feet, (B) facing the chest, (C) facing the side of the torso, (D) facing the top of the head and (E) facing the back. In all the five orientations the radar was 1 meter apart from the subject's body. From figure 8, we can observe that the lowest error rate for heart rate and breathing rate estimation is achieved when the radar faces the back of a subject's body. In other words, if user places the sensor underneath the bed, the performance of heat and breathing rate estimation might be maximized. Our result is in accordance with the findings in [30] where the authors explained that the accuracy of heart rate and breathing rate estimation from the back is maximized due to the minimal harmonic interference. Also we can observe that orientation A yields relatively smaller error rate. This could be attributed to the fact that the radar captures a larger profile of the abdomen than the chest, which exhibits more motion due to breathing and heartbeat in a supine position. Although different orientations yield different error rates, the overall error rate is within 3 CPM no matter where the sensor is placed.

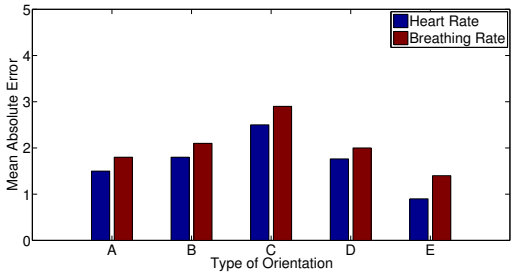

Figure 8: The performance of the heart and breathing rate estimation algorithm across different orientations in terms of mean absolute error measured using the unit of cycles (beats or breaths) per minute (CPM).

EVALUATING DOPPLESLEEP IN THE WILD

Data Collection

We recruited 8 healthy participants with no prediagnosed sleep disorders and collected sleep data for 2 sleep session each during their normal sleeping schedules at their homes. In total, we collected around 110 hours of sleep data. A biometric shirt (Hexoskin [9]) was provided to capture ground truth heart rate using embedded EKG electrodes, breathing rate using respiratory inductance plethysmography, and physical movement using accelerometer. Two commercially available sleep-sensing systems were provided to track sleep stages and serve as reference for sleep quality parameters. Zeo [7] is one such system that uses a headband embedded with EEG electrodes to track brain activity. Respironics [1] is another actigraphy-based system that predicts sleep stages based on accelerometer data. Both systems have been used in the research community as reasonably accurate references

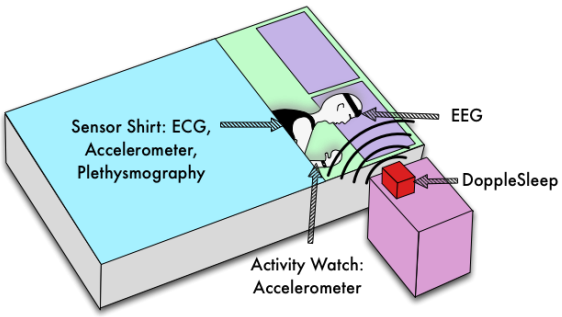

(a)

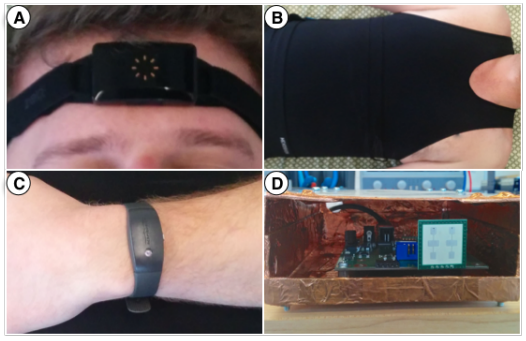

(b)

Figure 9: (a) illustrates the data collection setup where each participants sleeps in their natural sleeping place all the sensors. (b) shows all these sensor including Zeo EEG headband (A), Hexoskin biometric shirt (B), Actiwatch Activity tracker (C) and Doppler radar Sensor (D) used in our user study.

for wake/sleep and objective sleep quality parameters [22]. Each sensor's form factor and modalities are listed in table 1. Figure 9 shows the data collection setup, with biometric shirt, EEG headband, wristband sleep tracker and the proposed DoppleSleep system. Participants were instructed to place the Doppler radar sensor at least 0.5 meters away from the body. The radar module's sensitivity in horizontal and vertical direction is respectively 80 degree and 34 degree. As long as the body is within the radar's angular coverage, the radar can effectively capture any movement from the body.

Sensor name	Form Factor	Sensing Modalities
DoppleSleep	Contactless	Movement Heart Rate Breathing Rate
Hexoskin [9]	Biometric Shirt	3D Acceleration Heart Rate Breathing Rate
Zeo [7]	Headband	Electrical activity of brain
Actigraphy[1]	Wristwatch	Hand movements

Table 1: List of sensing devices used in the data collection

Validating Physical Activity Estimation

Here we evaluate DoppleSleep's movement classification algorithm against the ground truth estimation, in the wild.

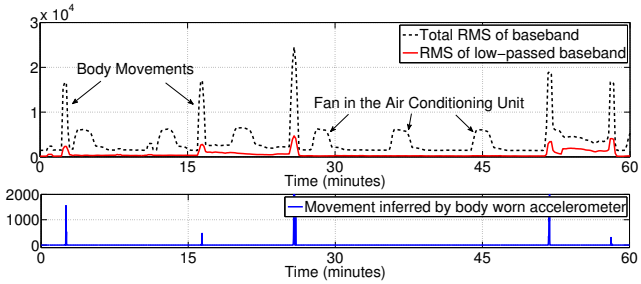

Figure 10: shows how the RMS energy of low-passed ($f_c = 3Hz$) baseband signal can successfully identify user's movement by successfully avoiding other bedroom vibrations (in this case a air conditioning unit). The total RMS energy of the baseband signal captures all the vibration present in user's sleeping environment.

The ground truth movement is estimated using a norm ($\sqrt{(a_x)^2 + (a_y)^2 + (a_z)^2}$) of 3D acceleration (a_x, a_y, a_z) averaged over a 30 second window from the accelerometer data in the wrist band. The movement estimation from the radar module is extracted from the RMS energy of the filtered baseband signal for the same 30 seconds. Figure 10 shows 60 minutes of estimated movement from the reference data and DoppleSleep for one sleep session. The peaks of the estimated movement using radar matches very well with the peaks of the reference movement. In this particular session, the air-conditioning unit in the participant's bedroom kicks in about every 10 minutes and the fan movement induces noise in the received signal: the peak in total RMS energy of baseband. Once, low pass filtered, the high frequency noise significantly reduces in energy. In order to objectively estimate the accuracy of physical movement estimation from the de-noised signal, we hypothesize that in a particular window, if the average of the norm of 3D accelerations of accelerometer worn by sleeper is greater than the median value, then the sleeper is physically active. Based on this hypothesis, we get the ground truth and classify sleeper's physical movement based on average RMS energy of baseband signal. Table 2 shows the confusion matrix of the activity vs. non-activity classification. It shows that with just one feature (average RMS energy of baseband), we could achieve reasonably good classification performance (about 86% average recall). These results indicate that the RMS energy of the low-passed baseband signal contains a lot of information about sleeper's physical movement.

		DoppleSleep	
		No Activity	Activity
Accelerometer	No Activity	85.8%	14.2%
	Activity	13.0%	87.0%

Table 2: The confusion matrix between the window-level (size 5 mins) prediction of sleeper's physical activity using the average RMS energy of low-passed baseband signal.

Validating Breathing and Heart Rate

We have already outlined the breathing and heart rate estimation algorithm in section "Sensing Breathing and Heart

Rate" and shown some primary results on the data collected in the laboratory environment. Here in figure 11a and 11b we show breathing rate and heart rate respectively collected from a participant during sleep from her natural sleep environment (non-laboratory settings). Signals from the EKG electrodes and RIP bands in the biometric shirt [9] are used as reference. Figure 11a and 11b show that the estimated breathing and heart rate time series closely follow the reference.

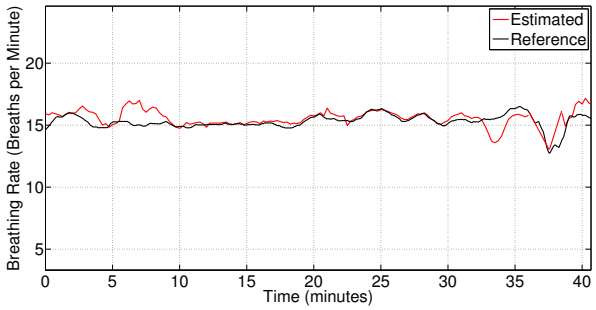

(a)

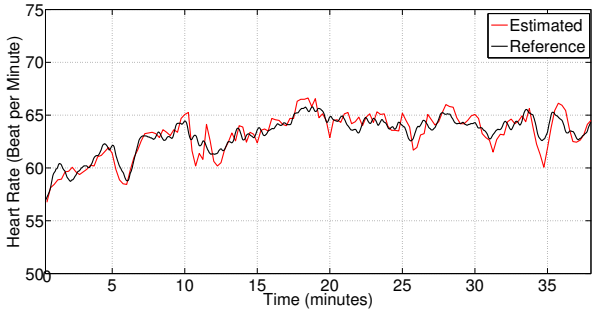

(b)

Figure 11: shows the reference and estimated (a) breathing rate (in breaths per minute) (b) heart rate (in beats per minute) of a participant collected during sleep.

Table 3 shows the error of our heart and breathing rate estimation algorithm across all the participants over the entire dataset. In addition to Mean Absolute Error (MAE) we used Normalized Root-Mean-Square Deviation (NMRSD) to calculate the error between the reference and estimated time series. NRMSD is a well-established metric that calculates the root-mean square of the error between the predicted and the reference time series and normalizes it by a dispersion measure of reference values. For example, the estimated heart rate for nth window is $HR_{est}(n)$ and the reference heart rate for every window is $HR_{ref}(n)$. The NRMSD is defined as:

$$NRMSD = \frac{\sqrt{\frac{\sum_{n=1}^{N}(HR_{est}(n)-HR_{ref}(n))^2}{N}}}{HR_{ref}max - HR_{ref}min} \quad (5)$$

If it is converted into a percentage ($NMRSD * 100\%$), it can be thought as a expected percent error measure from the reference. The results in table 3 suggests that the estimated heart rate is expected to be within 8.07% from the predicted value. Similarly the breathing rate estimation is expected to be within 10.84% of the reference value. The breathing error rate is slightly higher than the heart rate for our system. During sleep we almost always manifest slight movements that generates similar frequencies as the breathing process in the baseband, which has a negative affect on the breathing estimation algorithm. The results also indicate that DoppleSleep can track heart and breathing rate with a reasonable accuracy and can be sufficient for sleep modeling, if not for urgent medical diagnostic purposes.

	Breathing Rate	**Heart Rate**
MAE	1.98	3.29
NRMSD (%)	10.84	8.07

Table 3: The Mean Absolute Error (MAE) and Normalized Root-Mean-Square Deviation (NMRSD) of heart and breathing rate estimation.

SLEEP MODELING

The sleep inferences (sleep vs. wake state and REM vs. Non-REM stage) from the EEG headset (Zeo) are used as ground truth for modeling sleep. Our sleep modeling starts with a Sleep vs. Wake classifier, which is a primary requirement for any daily sleep tracking purposes. Once a particular epoch of data is identified as sleep, we then classify the epoch into two stages: REM and NREM (or Non-REM). Lastly we objectively estimate sleep quality using clinically validated sleep quality parameters.

Sleep vs. Wake Classifier

In order to train the Sleep vs. Wake classifier, we extract high-level features of the sleeper's physical activity, heart rate and breathing rate for every 5 minutes to predict sleep or wake states. We then apply different statistical functions to summarize various aspects of the activity, heart and breathing rate values in a frame. These statistical functions include extremes (min, max), averages (mean, RMS, median, quartiles), dispersion (standard deviation, interquartile range), peaks (number of peaks, average distance between peaks, average amplitude of peaks), rate of change (zero crossing rate) and shape (linear regression slope). This feature extraction process yields 42 frame-level features. As heart rate and breathing rate is only estimated during episodes of no physical movement, we apply spline interpolation to estimate missing heart rate and breathing rate values during these occasional episodes of movement. In order to find the most discriminative features for our Sleep vs. Wake classifier, we then apply a correlation-based feature selection (CFS) algorithm [23]. Figure 12a shows a scatter plot between two top frame-level features on the activity estimate. This suggests the presence a lot of body movements during wake state and little or no movement during sleep. Figure 12b shows that heart rate tends to decrease and reaches a resting value as we transition from wakefulness to sleep.

From the feature subset selected by our CFS algorithm for different combinations of low-level features (movement, heart rate and breathing rate estimates), we trained different classifiers that are listed in table 4. Using leave-one-subject-out

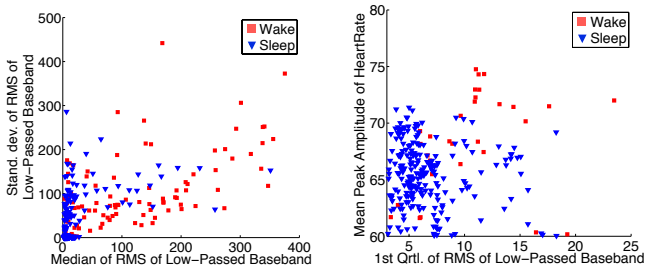

(a) (b)

Figure 12: (a) shows a scatter plot between two frame level features: median and standard deviation of RMS energy of the low-passed ($f_c = 3Hz$)baseband signal. (b) shows a scatter plot between the first quartile of RMS energy of the low-passed baseband and average amplitude of peaks of estimated heart rate.

cross-validation, we evaluated all these classifiers in terms of precision, recall and F-measure. From the results in table 4, we can observe that Random Forest outperforms all other classifiers with 89.3% precision, 89.6% recall and 89.1 % F-measure. When training the classifiers on just movement estimates (Mo) the performance decreases to 86.0% precision, 86.5% recall and 86.2 % F-measure. This clearly indicates that vital signal estimation (both breathing rate, Br and heart rate, Hr) carries discriminative features that enhance the performance of the classifier. Lastly the comparison between performance of two Random Forest classifiers: one trained on just vital estimates (Br and Hr) and the other on just movement (Mo) estimates, suggests that movement estimation (Mo) plays a more significant role in this Sleep vs. Wake classification.

Features	Classifier	P (%)	R (%)	F (%)
Mo+Br+Hr	Naive Bayes	82.3	83.5	81.3
Mo+Br+Hr	Logistic Regression	83.1	84.2	82.3
Mo+Br+Hr	SVM	83.1	84.2	82.3
Mo+Br+Hr	Random Forest	89.3	89.6	89.1
Mo	Random Forest	86.0	86.5	86.2
Br+Hr	Random Forest	77.8	80.4	75.9

Table 4: Sleep vs. Wake classification performance with different classifiers with different sets of features selected by CFS feature selection from different combination of low-level feature sets consisting radar-based movement (Mo), breathing rate (Br) and heart rate (Hr) estimates in terms of precision (P), recall (R) and f-measure (F).

Sleep Stage (REM vs. Non-REM) Classifier

While Sleep vs. Wake classification provides an estimate on the amount of sleep a person gets, further classification of sleep stages or sleep stage mining can indicate the quality of sleep or how restorative the sleep was. To this end, we developed a binary sleep stage classifier that disambiguates REM and NREM stages for episodes/epochs that are predicted as sleep by the Sleep vs. Wake classifier. We used the same feature extraction and selection process as the Sleep vs. Wake classifier training. Table 5 shows the effect of low-level features and classifiers on the performance. Random Forest based classifier trained on all the three modalities (movement, heart rate and breathing rate), outperforms all the other classifiers with 80.5% precision, 80.2% recall and 80.2 % F-measure. Only using features extracted from movement estimates, reduces the performance to 75.5% precision, 75.4% recall and 75.8% F-measure. This illustrates that high-level features extracted from breathing and heart rate estimation provide more complementary information for REM vs. NREM than for Sleep vs. Wake classification.

Features	Classifier	P (%)	R (%)	F (%)
Mo+Br+Hr	Naive Bayes	73.8	64.2	60.5
Mo+Br+Hr	Logistic Regression	71.8	71.7	71.6
Mo+Br+Hr	SVM	76.1	74.2	75.3
Mo+Br+Hr	Random Forest	80.5	80.2	80.2
Mo	Random Forest	75.5	75.4	75.8
Br+Hr	Random Forest	62.8	64.4	62.9

Table 5: REM vs. Non-REM classification performance with different classifiers with different sets of features selected by CFS feature selection from different combination of low-level feature sets consisting radar-based movement (Mo), breathing rate (Br) and heart rate (Hr) estimates in terms of precision (P), recall (R) and f-measure (F).

Objective Sleep Quality Measurement

Summarizing a sleep session using a validated set of objective sleep quality measures can intuitively inform users of their sleep quality and aid in taking corrective measures such as improving sleep hygiene if needed. It also facilitates establishment of long-term trends in sleep quality. In this study we used 4 well-established sleep quality measures to summarize a sleep session. Figure 13 shows how sleep quality parameters are estimated from DoppleSleep's sleep vs. wake inference.

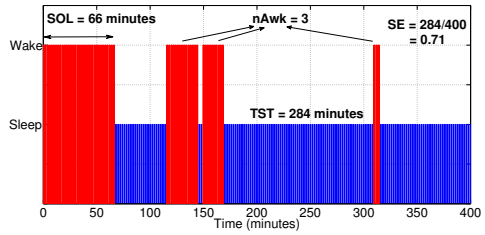

Figure 13: Illustration of objective sleep quality estimation.

(i) *Sleep Onset Latency (SOL)* is defined as the time taken to transition from being fully awake to being asleep. Abnormally large SOL values indicate insomnia and small SOL values indicate sleep deprivation. From figure 13, we can infer that the participant took about an hour to transition from wake to sleep. (ii) *No. of Awakenings (NAwk)* indicates the total number of transitions from sleep to wake in a particular sleep session [14]. It is another significant sleep metric that is linked with sleep apnea, disruption in circadian cycle, insomnia etc. Our participant has 3 arousal events: two long awake segments and a third brief event. (iii) *Total Sleep Time (TST)* is a measure of the total time duration that someone

spends in sleep state in a particular sleep session. This equals to the length of sleep session minus wake time. In figure 13, the total wake time (284 mins) was subtracted from the length of sleep session (400 mins) resulting in a TST of 284 minutes. (iv) *Sleep Efficiency (SE)* is the ratio between total sleep time (TST) and total length of sleep session. It summarizes the three previous metrics. Reduced Sleep efficiency (below 85%) is indicative of sleep disorders since initiating (high SOL), and maintaining sleep (high NAwak and low TST) tend to be difficult. Figure 13 shows that our participant's TST was 284 minutes and total bed time was about 400 minutes resulting in sleep efficiency (SE) of 71%. A Pearson correlation coefficient analysis between the SOL, NAwk and SE estimated by DoppleSleep and by the ground truth reveals relatively high correlation (0.83, 0.69 and 0.78).

DOPPLESLEEP SYSTEM IMPLEMENTATION

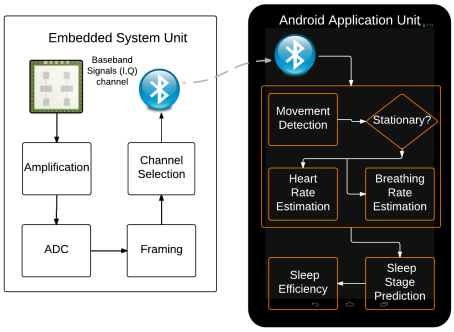

(a)

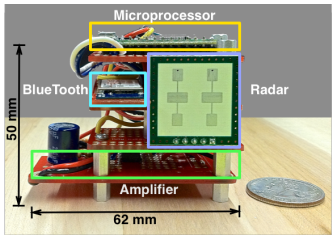

(b)

Figure 14: shows (a) overview of the DoppleSleep system implementation. (b) the embedded systems unit of DoppleSleep.

Figure 14a shows an overview of DoppleSleep consisting of an embedded system unit and an Android smartphone unit. The embedded system comprises of an off-the-shelf K-band (24 GHz) short-range doppler radar module[12]. Although the module has an in-built low noise amplifier to boost the I and Q baseband signals, we found that the output signals of the radar needed further amplification before sampling by an ADC. We used a dual channel, non-inverting op-amp and set the gain to 11 times. After amplification we used a Teensy 3.1 Microcontroller [4] with an ADC of 16 bit resolution to sample the signal. The amplified baseband signals were sampled at a 1kHz. The sampled data was stored in a circular buffer and the optimal channel was selected by measuring the interquartile range. The signal was then framed (containing 1024, 16-bit values) and transmitted through a bluetooth unit, BlueSMirf Silver [5]). The Bluetooth modem ensures reliable wireless connectivity with the Android device up to a distance of 18 meters. Figure 14b illustrates different parts of the embedded system unit. The Android application unit buffers the asynchronous frame-by-frame data received from the embedded unit via Bluetooth. It then runs the physical activity, heart rate and breathing rate estimation algorithms, classifies sleep stages estimates sleep quality.

The radar module consumes 28.5mA at 5V (0.1425W), the bluetooth module and microprocessor consume 102mA at 5V (0.3675W), and the amplifier consumes 4mA at 9V (0.036W). The total power consumption of the DoppleSleep system comes out to be 0.546W while connected and transferring data. The DoppleSleep Android application consumes 0.471W of power and utilizes 2.11% of the CPU.

HEALTH CONSIDERATIONS

Federal regulation limits the continuous exposure of wireless signal to $1mW/cm^2$ of skin surface to be harmless. At a $distance > 19cm$ from a 24 GHz radar transceiver with an output power of 100mW and an opening angle of $80X35$, the power per cm^2 surface drops below 1mW. Thus, DoppleSleep has no health implications for continuous use in a home.

CONCLUSION AND FUTURE WORK

In this paper, we have described the design, implementation, and evaluation of DoppleSleep - a contactless sleep sensing system that facilitates continuous and unobtrusive long-term sleep monitoring using a single Doppler radar sensor. DoppleSleep tracks an individual's physical body movements, heart beat and breathing during sleep, and objectively infers of sleep quality. We have validated the feasibility of DoppleSleep in a lab setting and in the wild and our results show that DoppleSleep can detect physical movements with 86% recall rate, and estimate heart and breathing rate with an error rate of 8.07% and 10.84% respectively. Based on our results, by combining vital signal estimation with movement tracking, DoppleSleep shows great promise for continuous, passive, unobtrusive sleep monitoring in real-world settings with 89.6% recall for Sleep vs. Wake and 80.2% recall for REM vs. Non-REM classification.

There are many areas for further exploration in sleep stage mining using vital signals. Since PSG is considered as the medical gold standard for sleep stage mining, we are currently working on validating the system in clinical settings against PSG. This also provides an opportunity to test the efficacy of DoppleSleep in diagnosing sleep related disorders in patients suffering from sleep apnea. We are also working on extending DoppleSleep to continuously track vital signals as well as movement from multiple individuals in a bedroom. In order to do so we are considering implementing an radar array to triangulate reflections from different persons.

ACKNOWLEDGMENTS

This work has been partially supported by the following grants: NSF IIS-1202141, NSF IIS-1344587, NSF CBET-1343058, NSF IIS-1344613 and Intel Science and Technology Center on Pervasive Computing (ISTC-PC).

REFERENCES

1. http://actigraphy.respironics.com.
2. http://science.education.nih.gov/supplements/nih3/sleep.
3. https://jawbone.com/up.
4. https://www.pjrc.com/store/teensy31.html.
5. https://www.sparkfun.com/products/10269.
6. http://www.aastweb.org/resources/guidelines/standardpsg.
7. http://www.digifit.com/zeo/.
8. http://www.fitbit.com.
9. http://www.hexoskin.com.
10. http://www.itamarmedical.com/watchpat.
11. http://www.nhlbi.nih.gov/health/health-topics/topics/sdd/why.
12. http://www.rfbeam.ch/products/k-lc5-transceiver/.
13. http://www.withings.com/us/withings-aura.
14. Akerstedt, T., Billiard, M., Bonnet, M., Ficca, G., Garma, L., Mariotti, M., Salzarulo, P., and Schulz, H. Awakening from sleep. *Sleep Medicine Reviews 00*, 0 (2002), 1–19.
15. C. Iber et al. The american academy of sleep medicine manual for the scoring of sleep and associated events. *American Academy of Sleep Medicine* (2007).
16. Chen, K.-M., Huang, Y., Zhang, J., and Norman, A. Microwave life-detection systems for searching human subjects under earthquake rubble or behind barrier. *Biomedical Engineering, IEEE Transactions on 47*, 1 (2000), 105–114.
17. Choe, E. K., Consolvo, S., Watson, N. F., and Kientz, J. A. Opportunities for computing technologies to support healthy sleep behaviors. In *Proceedings of the SIGCHI Conference on Human Factors in Computing Systems*, ACM (2011), 3053–3062.
18. de Souza, L., Benedito-Silva, A. A., Pires, M. N., Poyares, D., Tufik, S., Calil, H. M., et al. Further validation of actigraphy for sleep studies. *SLEEP-NEW YORK THEN WESTCHESTER 26*, 1 (2003), 81–85.
19. Droitcour, A., Boric-Lubecke, O., Lubecke, V., Jenshan, L., and Kovacs, G. Range correlation and i/q performance benefits in single-chip silicon doppler radars for noncontact cardiopulmonary monitoring. *Microwave Theory and Techniques, IEEE Transactions on 52*, 3 (March 2004), 838–848.
20. Droitcour, A. D., and O Lubecke, V. 0.25 μm cmos and bicmos single-chip direct-conversion doppler radars for remote sensing of vital signs. *Solid-State Circuits* (2002).
21. Ebrahimi, F., Mikaeili, M., Estrada, E., and Nazeran, H. Automatic sleep stage classification based on eeg signals by using neural networks and wavelet packet coefficients. In *Engineering in Medicine and Biology Society, 2008. EMBS 2008. 30th Annual International Conference of the IEEE* (Aug 2008), 1151–1154.
22. Gu, W., Yang, Z., Shangguan, L., Sun, W., Jin, K., and Liu, Y. Intelligent sleep stage mining service with smartphones. In *Proceedings of the 2014 ACM International Joint Conference on Pervasive and Ubiquitous Computing*, UbiComp '14 (2014), 649–660.
23. Hall, M. A. Correlation-based Feature Selection for Machine Learning. *PhD Thesis* (April 1999).
24. Hao, T., Xing, G., and Zhou, G. isleep: Unobtrusive sleep quality monitoring using smartphones. SenSys '13 (2013), 1–14.
25. Jain, V., Mytri, V., Shete, V., and Shiragapur, B. Sleep stages classification using wavelettransform amp; neural network. In *Biomedical and Health Informatics (BHI), 2012 IEEE-EMBS International Conference on* (Jan 2012), 71–74.
26. Kay, M., Choe, E., Shepherd, J., Greenstein, B., Watson, N., Consolvo, S., and Kientz, J. Lullaby: A capture & access system for understanding the sleep environment. Ubicomp (2012).
27. Li, C., Cummings, J., Lam, J., Graves, E., and Wu, W. Radar remote monitoring of vital signs. *Microwave Magazine, IEEE 10*, 1 (2009), 47–56.
28. Li, C., and Lin, J. Complex signal demodulation and random body movement cancellation techniques for non-contact vital sign detection. In *Microwave Symposium Digest, 2008 IEEE MTT-S International* (June 2008), 567–570.
29. Li, C., Lubecke, V. M., Boric-Lubecke, O., and Lin, J. A review on recent advances in doppler radar sensors for noncontact healthcare monitoring. *Microwave Theory and Techniques, IEEE Transactions on 61*, 5 (2013), 2046–2060.
30. Li, C., Xiao, Y., and Lin, J. Experiment and spectral analysis of a low-power ka -band heartbeat detector measuring from four sides of a human body. *Microwave Theory and Techniques, IEEE Transactions on 54*, 12 (Dec 2006), 4464–4471.
31. Li, C., Xiao, Y., and Lin, J. Design guidelines for radio frequency non-contact vital sign detection. In *Engineering in Medicine and Biology Society, 2007. EMBS 2007. 29th Annual International Conference of the IEEE*, IEEE (2007), 1651–1654.
32. Lin, J. C. Noninvasive microwave measurement of respiration. *Proceedings of the IEEE 63*, 10 (Oct 1975), 1530–1530.
33. Lohman, B., Boric-Lubecke, O., Lubecke, V., Ong, P., and Sondhi, M. A digital signal processor for doppler radar sensing of vital signs. *Engineering in Medicine and Biology Magazine, IEEE 21*, 5 (2002), 161–164.

34. Park, B.-K., Boric-Lubecke, O., and Lubecke, V. Arctangent demodulation with dc offset compensation in quadrature doppler radar receiver systems. *Microwave Theory and Techniques, IEEE Transactions on 55*, 5 (May 2007), 1073–1079.

35. Sadeh, A. The role and validity of actigraphy in sleep medicine: an update. *Sleep medicine reviews 15*, 4 (2011), 259–267.

36. Sadeh, A., Hauri, P., Kripke, D., and Lavie, P. The role of actigraphy in the evaluation of sleep disorders. *Sleep 18*, 4 (1995), 288–302.

37. Verster, J., Pandi-Perumal, S., and Streiner, D. *Sleep and quality of life in clinical medicine*. Springer, 2008.

38. Xiao, Y., Lin, J., Boric-Lubecke, O., and Lubecke, V. Frequency-tuning technique for remote detection of heartbeat and respiration using low-power double-sideband transmission in the ka-band. *Microwave Theory and Techniques, IEEE Transactions on 54*, 5 (May 2006), 2023–2032.

39. Xiao, Y., Lin, J., Boric-Lubecke, O., and Lubecke, V. M. Frequency-tuning technique for remote detection of heartbeat and respiration using low-power double-sideband transmission in the ka-band. *Microwave Theory and Techniques, IEEE Transactions on 54*, 5 (2006), 2023–2032.